J. Fluid Mech. (2013), *vol.* 717, *pp.* 347–360.
doi:10.1017/jfm.2012.575

On the measurement of the turbulent diffusivity of a large-scale magnetic field

S. M. Tobias[1],† and F. Cattaneo[2]

[1]Department of Applied Mathematics, University of Leeds, Leeds LS2 9JT, UK

[2]Department of Astronomy and Astrophysics and The Computation Institute, University of Chicago, Chicago, IL 60637, USA

(Received 1 August 2012; revised 28 September 2012; accepted 16 November 2012; first published online 1 February 2013)

We argue that a method developed by Ångström (*Ann. Phys. Chem.*, vol. 114, 1861, pp. 513–530) to measure the thermal conductivity of solids can be adapted to determine the effective diffusivity of a large-scale magnetic field in a turbulent electrically conducting fluid. The method consists of applying an oscillatory source and measuring the steady-state response. We illustrate this method in a two-dimensional system. This geometry is chosen because it is possible to compare the results with independent methods that are restricted to two-dimensional flows. We describe two variants of this method: one (the 'turbulent Ångström method') that is better suited to laboratory experiments and a second (the 'method of oscillatory sines') that is effective for numerical experiments. We show that, if correctly implemented, all methods agree. Based on these results we argue that these methods can be extended to three-dimensional numerical simulations and laboratory experiments.

Key words: MHD and electrohydrodynamics, MHD turbulence, turbulent mixing

1. Introduction

The evolution of astrophysical magnetic fields is most often characterized by changes in their large-scale structure. This is typically because the small-scale magnetic fields are not amenable to direct observations. The large-scale evolution is often described using the concept of turbulent diffusion (see e.g. Parker 1979). This is justified by noting that most astrophysical plasmas have very large Reynolds numbers and are in a state of vigorous turbulent motion. Although this concept has proven useful, its precise theoretical underpinning has remained elusive. The reasons for the difficulties are twofold. The first is that the magnetic field is a vector quantity so its transport properties are more akin to (although subtly different from) vorticity rather than temperature. The second is that the magnetic field is not a passive quantity and so it can effect the underlying turbulence through the action of the Lorentz force.

Analytical approaches to determining the turbulent diffusivity are difficult; they can only be justified in certain regimes such as low-Reynolds-number flows or short correlation time turbulence, which are not the correct regimes for astrophysical flows (Moffatt 1978; Krause & Raedler 1980). However, even if these assumptions are made,

† Email address for correspondence: smt@amsta.leeds.ac.uk

the biggest difficulty lies in self-consistently calculating the effect of the magnetic field once it becomes dynamic and modifies the statistics of the underlying turbulence. Much of what is known (or not known) derives from measurements of the turbulent diffusivity in numerical experiments (see e.g. Cattaneo & Vainshtein 1991; Cattaneo 1994; Courvoisier, Hughes & Tobias 2009). Even these are not entirely straightforward. The first issue arises owing to the requirement for a separation of scales between the characteristic scale of the underlying turbulence and the (much-larger) scale on which the magnetic field displays diffusive behaviour. The second is that the magnetic Reynolds number needs to be large enough for a clear distinction between the collisional and turbulent diffusion. This is not only numerically challenging but also introduces large fluctuations that somehow need to be controlled (Cattaneo & Hughes 2009). Finally in three dimensions, the vectorial nature of the magnetic field introduces the possibility of dynamo action, whereby the large-scale magnetic field is not only advected and diffused but also amplified. This makes it difficult to disentangle the effects of diffusion from mean induction. These issues notwithstanding there are methods that have been constructed in order to calculate the turbulent diffusivities in numerical experiments (Brandenburg *et al.* 2008; Brandenburg, Svedin & Vasil 2009). Recently another possibility has emerged, which is to measure the turbulent diffusivity in laboratory experiments based on liquid metals (see Monchaux *et al.* 2009). Indeed there have been a couple of implementations to calculate the turbulent diffusivity for an experiment in toroidal geometry (Frick *et al.* 2010; Noskov *et al.* 2012). Most of the methods that have been used to calculate the turbulent diffusivity in numerical experiments do not carry over to experimental set-ups. For example, the popular 'test field method' (Schrinner *et al.* 2005) involves the solution in space and time of an auxiliary field (the test field) that cannot be reproduced in a real experiment.

In this paper we argue that a popular technique due to Ångström (1861), yes, really, *that* Ångström, for measuring the thermal diffusivity in solids can be adapted to measure the turbulent diffusivity of a magnetic field in an electrically conducting fluid. We shall describe two variants of this technique. One, which we term the TAM is suitable for laboratory experiments, whilst the second, the 'method of oscillatory sines' (MOS), is better suited to numerical experiments. The most important feature of these methods is that they are based on measuring properties of the magnetic field in a stationary state. We believe that this is desirable because it leads to the property that by taking enough measurements (or measurements for long enough) one can reduce the errors to an acceptable level.

In the long term, we would like to use these methods to address some fundamental issues: under what circumstances does it make sense to characterize the evolution of the magnetic field in terms of a turbulent diffusion? If it does make sense, then what is the value of the turbulent diffusivity, how does it differ from that of a passive scalar and what is its dependence on magnetic field strength. In this paper we examine the basic concepts and apply the methods to turbulent flows in two dimensions. This will act as a proof of concept. Because other methods are available to measure the diffusivity in two dimensions we can compare these new methods and determine under what circumstances agreement is reached. In a further paper we shall extend the methods to the more interesting case of three-dimensional turbulence.

2. Measurement of the turbulent diffusivity

There are two related, but separate, concepts of turbulent diffusion that are generally invoked. The first, termed Richardson diffusion (Richardson 1926), looks at the

process of diffusion of scales that are comparable with the range of scales of the inertial range of the turbulence; for an extension of the concept of Richardson diffusion to vector fields see (Eyink 2009). In this case there are always scales of motion that are larger than the scales at which the diffusion is operating. The other, termed Taylor diffusion (Taylor 1921) (which is the subject of this paper), arises in cases where there is a separation of scales between the random motions (such as the fluid turbulence) and the dynamics of large scales of the quantity of interest. If this separation exists, and subject to reasonable assumptions about the nature of the underlying turbulent velocity, then the evolution of the average over scales much larger than that characterizing the turbulent velocity can be described using an effective diffusivity, which, in general, should be independent of collisional processes. It is possible for the diffusivity to be time-dependent, but here we restrict attention to the case where the flows are statistically steady and so the diffusivity is independent of time. For a scalar quantity, such as temperature or contaminant, measurement of the effective diffusivity is straightforward. It can be calculated either by prescribing the large-scale variation of the scalar and measuring its rate of decay (Cattaneo & Vainshtein 1991) or alternatively by calculating the trajectories of the turbulent flow and utilizing the result that the turbulent diffusivity is related to the time rate of change of the mean-square displacement (Taylor 1921; Cattaneo 1994). For anisotropic cases the calculation is less straightforward, but in any case, knowledge of the two-point statistics yields all the information required to determine the diffusivity tensor. Because in two dimensions the magnetic field can be described by the evolution of a single scalar field, either one of these two methods can be immediately utilized to calculate the turbulent diffusivity, whether or not the magnetic field is active or passive.

In the case of a vector quantity the calculation is more involved, because now there is the possibility of dynamo action which leads to the amplification of magnetic energy. Therefore, imposing an initial large-scale distribution of magnetic field and waiting for it to evolve to measure its rate of decay may prove a fruitless exercise; it may actually grow. Indeed, for high magnetic Reynolds number, if the flow is sufficiently complicated to lead to a turbulent diffusivity it is almost guaranteed to lead to dynamo action, where the field grows until it reaches a stationary state. There are ways of circumventing the problem of the lack of decay. For example, the test-field method attempts to measure the turbulent diffusivity of the stationary state. Its aim is to disentangle the effects of induction from those of diffusion by calculating the evolution of a test field that satisfies an auxiliary fluctuating vector field equation (the test field). Although the test-field method has been used extensively in numerical work, it is hard to see how it may be used directly in the laboratory. Moreover, the expression for the turbulent diffusivity in terms of trajectories for a vector field is significantly more complicated than for a scalar (Moffatt 1974). It has a piece that requires the determination of the two-point statistics of the displacement field and also a piece that requires the knowledge of the Lagrangian gradient of the displacement field. In a chaotic flow, this quantity is related to the Lyapunov exponents and therefore increases exponentially in time (or faster if it is in the inertial range scales), even in a stationary flow (Moffatt 1978). It is therefore almost impossible to implement trajectory methods for vector fields even numerically, let alone experimentally.

2.1. *A simple one-dimensional example*

The considerations described above, lead us to the conclusion that the method for calculating the turbulent diffusivity should be based on measurements in a stationary

state (i.e. not decay), should not use trajectories and should not rely on fictitious fields. We take as our starting point the method proposed by Ångström for calculating the thermal diffusivity of a one-dimensional metal rod. The essence of the method can be illustrated very simply. Imagine a metal rod with one end kept at fixed temperature whilst the other end is periodically (sinusoidally) heated and cooled with frequency ω. After a sufficiently long time so that the transients that are related to the initial distribution of temperature in the rod have died away, the temperature at any point within the rod will vary sinusoidally in time with frequency ω and with an amplitude that and phase that depend on the thermal diffusivity of the rod (assuming that the thermal diffusivity does not depend on temperature). Thus, if one could measure either of these quantities then one could invert the problem and infer the thermal diffusivity.

Now imagine that instead of a solid rod, we have a very long thin pipe filled with some fluid. We further imagine that the fluid in this pipe is turbulent with a typical eddy size comparable with the diameter of the pipe. Once again, one end of the pipe is kept at $T = 0$ whilst the other is heated and cooled sinusoidally. What would be the outcome of the experiment described above? The temperature at each point along the pipe is the superposition of two signals, one at the frequency ω which arises owing to the oscillation at the boundary and another component that arises because of the turbulent fluctuations. If the frequency of the turbulence is large compared with that of the oscillation then it is possible to measure the amplitude of the sinusoidal component to a required level of precision by taking a very long signal. What is crucial here is that both the turbulence and the system are in a statistically stationary state, so there is no restriction *a priori* to the length of signal that can be taken.

We conclude this section by noting that, from a numerical point of view, by sticking two of these problems together we may map a non-periodic system with a time-dependent boundary condition into a spatially periodic system with an oscillatory source term. If this source term is spatially localized then the new system is a good model of a boundary driven experiment, we call this technique the TAM. However, now that we are in the realm of numerics we are not restricted to localized source terms and so one may consider oscillatory sources that are sinusoidal in space, which as we shall see has some advantages; we term this type of calculation the MOS. Although this example is 'one-dimensional', the techniques can clearly be extended to a volume of turbulent fluid by an appropriate distribution of sources and sinks.

3. Mathematical formulation and measurement techniques

Our objective is to construct a simple model and apply the techniques described above to determine under what circumstances the turbulent diffusivity can be calculated. Our computational domain is a two-dimensional Cartesian rectangle ($0 \leqslant x < X_{max},\ 0 \leqslant y < Y_{max}$). For computational convenience we apply periodic boundary conditions in x and y. The interaction between an incompressible fluid and a magnetic field in two dimensions can be described in terms of two quantities, the vertical component of the vorticity ζ and the flux function A. The evolution equations for these quantities are

$$\partial_t \zeta = J(\psi, \zeta) + J(A, \nabla^2 A) + \nu \nabla^2 \zeta - \Lambda \zeta + G_0, \tag{3.1}$$

$$\partial_t A = J(\psi, A) + \eta \nabla^2 A + S_A, \tag{3.2}$$

where $J(a, b) = a_x b_y - a_y b_x$, $\nu = 5 \times 10^{-4}$ is the viscosity, $\eta = 10^{-3}$ is the collisional diffusivity and $\Lambda = 3 \times 10^{-2}$ is the coefficient of friction. Here $G_0(x, y, t)$ is the driving (sometimes referred to as the force curl) and S_A is the source term for the flux

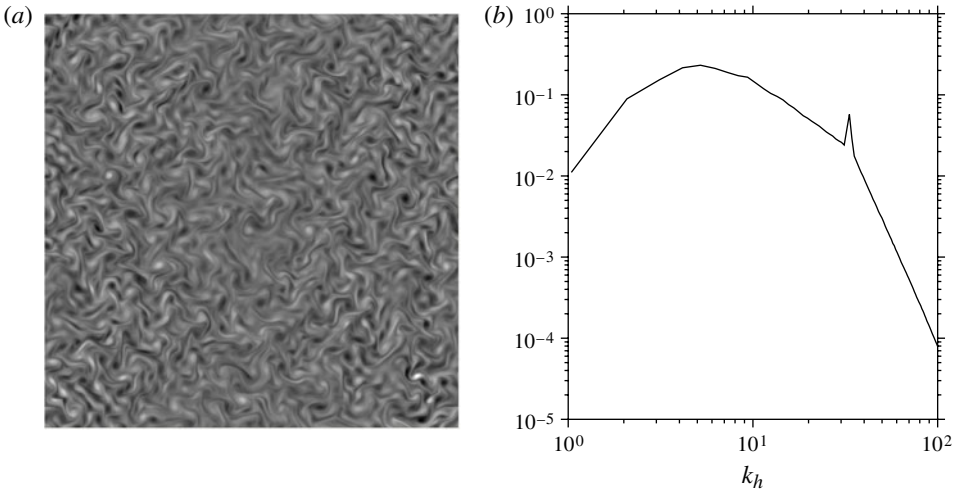

FIGURE 1. (*a*) Density plot of vorticity as a function of x and y at a representative time for a kinematic case. (*b*) Time-averaged energy spectrum. The narrow peak corresponds to the scale of the forcing whilst the broad plateau arises at a scale where the inverse cascade is balanced by friction.

function. The vorticity is related to the streamfunction by $\zeta = -\nabla^2\psi$ and the magnetic field $\boldsymbol{B}$ is given by $\boldsymbol{B} = (-A_y, A_x)$.

3.1. *Construction of the velocity*

In order to make meaningful measurements of the turbulent diffusion, there are certain characteristics that the velocity field should possess. It should be stationary, it should be complicated (in the sense that it should have positive Lyapunov exponents everywhere) and it should satisfy the requirement of scale separation both in space and time. Interestingly this can be achieved trivially in three dimensions by going to high enough Reynolds number, but is somewhat trickier to achieve in two dimensions. The main issue is the presence of an inverse cascade that has a tendency to generate large, long-lived eddies; this breaks scale separation in both space and time. The simplest way to control this is to introduce friction, which we do by setting $\Lambda > 0$. This removes the energy at large scales and ensures that a stationary solution can be achieved. The forcing is chosen to be localized in phase space to a band of high wavenumbers so that the corresponding velocity is likewise characterized by high(ish) wavenumbers. The amplitude and renewal time for the forcing are selected so that the resulting eddies have lifetimes that are comparable with their turnover times. This requires some tuning of the parameters. There are many different ways of selecting the forcing. Our procedure involves selecting a wavenumber to force from a band of wavenumbers $15 \leqslant k_x, k_y \leqslant 20$ and maintaining the forcing for a length of time (the renewal time) that is itself chosen from a uniform (top-hat) distribution with well-defined mean and width, before selecting another wavenumber to force. We have determined, however, that the statistics and dynamics of the resulting velocity is not sensitive to the precise form of this forcing. The friction is selected so as to remove energy at small wavenumbers. We solve (3.1)–(3.2) using standard pseudospectral techniques (Canuto *et al.* 1987) and all calculations are performed at a resolution of 1024^2.

Figure 1(*a*) shows a snapshot of the vorticity after it has reached a statistically steady state. Here we have set $X_{mx} = Y_{mx} = 4\pi$ with a renewal time of $\tau_r = 0.1$; these parameters are held fixed for the rest of the paper. The field is characterized by the presence of many interacting vortices with a well-defined characteristic spatial scale, which is not too large. Figure 1(*b*), which gives a two-dimensional spectrum of the kinetic energy, shows that the solution is dominated by two wavenumbers, one at the forcing scale, but a significant amount of energy has inverse cascaded to lower wavenumbers with a peak in energy at $k_h = (k_x^2 + k_y^2)^{1/2} \sim 5$. This peak is determined by a balance between the inverse cascade efficiency and the friction. The temporal coherence of the flow can be characterized by the correlation time τ_c. For these parameters $\tau_c \approx 0.7$, which is significantly larger than the renewal time τ_r of the forcing. The increased correlation time of the flow is due to the presence of longer-lived coherent vortices that emerge as a result of nonlinear interactions in the flow.

3.2. *Description of the experiments*

3.2.1. *The measurement of turbulent diffusivity*

At this point, we need to be more precise about what is meant by turbulent diffusivity. The idea is that even though the evolution of B_x is described by (3.2), the evolution of the averages of B_x is described by

$$\partial_t \overline{B_x} = \eta_T \nabla^2 \overline{B_x} + \overline{S}, \tag{3.3}$$

where η_T is the turbulent diffusivity and $\overline{S}$ is some average version of S. The type of average depends on circumstances; in principle, they could be time averages, ensemble averages or spatial averages. Here we consider spatial averages over volumes that are small compared with the system size, but large compared with a typical length scale for the turbulent eddies.

The subject of homogenization theory is to calculate η_T given the velocity, without ever calculating B_x. What we want to do here is different. Here, we want to measure η_T, i.e. we solve (3.2) and then use the solution for B_x to say what value of η_T best describes the evolution of $\overline{B_x}$.

We outline four different ways of doing this for two-dimensional flows; the first two of which are well-tested and understood and are included here for comparison. The first method involves setting $S = 0$ and prescribing an initial field with only a large-scale component and no net flux so that $B_x(t = 0) = B_0 \sin(2\pi y/Y_{mx})$. The turbulent diffusivity can be calculated from the decay rate of the amplitude of the largest-scale Fourier component. For this case $B_x(t)$ is not stationary, it is a decaying field. Hence, if one wanted to improve the accuracy of the measurement then one would need to repeat the experiment a number of times to reduce the error. Furthermore, as B_x decays the value of η_T changes (since η_T depends on the field strength), which can make unambiguous calculation of η_T difficult.

A slightly different method that takes care of the problem of non-stationarity is to impose a uniform field (i.e. B_x independent of y). For this case the initial value of $\overline{B}_x$ is preserved and the system evolves to a stationary state. Now, the turbulent diffusivity can not be calculated by measuring a decay rate, as nothing decays. However, it can easily be shown that in two dimensions (see e.g. Zel'dovich 1957; Gruzinov & Diamond 1994)

$$\frac{\eta_T}{\eta} = \frac{\overline{B^2}}{\overline{B}^2}, \tag{3.4}$$

and that this remains true even when the average is taken over the whole spatial domain so that the relationship becomes

$$\frac{\eta_T}{\eta} = \frac{\overline{B^2}}{B_0^2}. \tag{3.5}$$

Because the measurements are taken over a stationary ensemble, the determination of the turbulent diffusivity can be made as accurate as required by averaging over a sufficiently long time scale. However, because of the possibility of dynamo action, neither this method nor the previous one can be generalized to three dimensions in a straightforward way.

The next two methods use a stationary ensemble and should be generalizable to three dimensions. For these methods it is necessary that S be non-zero and a stationary, but not a steady function of time. The two methods differ solely in the localization of the spatial part of S. The idea is to compare the average solutions of (3.2) with the solutions of the averaged (3.3) to find the value of η_T that yields the best agreement. The critical question is then, which aspects of the solutions to these equations should be compared. To address this issue, we shall examine the specific case where S is given by

$$S = \omega B_0(y) \cos \omega t, \tag{3.6}$$

where the factor of ω is introduced for normalization purposes. The corresponding $\overline{S}$ is unknown, as it is the result of spatial averaging of S. However, it is reasonable to assume that it has the same frequency dependence in time as S. The solution of (3.3) can be written in terms of Fourier series as

$$\sum_{k_x,k_y} \phi(k_x, k_y, t) \exp \mathrm{i}(k_x x + k_y) + c.c., \tag{3.7}$$

where the coefficients are given by

$$\phi(k_x, k_y, t) = \omega \hat{S}(k_y) \,\mathrm{Re}\left[\frac{\exp(\mathrm{i}\omega t)}{\eta_T\left(k_x^2 + k_y^2\right) + \mathrm{i}\omega}\right] + C \exp\left(-\eta_T\left(k_x^2 + k_y^2\right) t\right), \tag{3.8}$$

where $\hat{S}(k_y)$ is the Fourier coefficient of $\overline{B_0}$. The transient response decays exponentially in time and is determined by the initial conditions, thus could be made zero by a suitable choice. Note that since the source is independent of x and therefore $\overline{B_0}$ is independent of x it makes sense to focus on the $k_x = 0$ coefficients which are given by

$$\phi(k_y, 0, t) = G(k_y) \cos(\omega t - \psi) \tag{3.9}$$

where ψ is a phase and $G(k_y)$ is the Fourier coefficient of the time-periodic response for $k_x = 0$, which is given by

$$G(k_y) = \frac{\omega \hat{S}(k_y)}{\left(\eta_T^2 k_y^4 + \omega^2\right)^{1/2}}. \tag{3.10}$$

In principle, one can use equation (3.9) to calculate η_T if $\hat{S}(k_y)$ were known. As noted earlier, it is not. However, if one were to consider solutions of equation (3.9) for two different driving frequencies, ω_1 and ω_2 say, then the ratio of these coefficients at

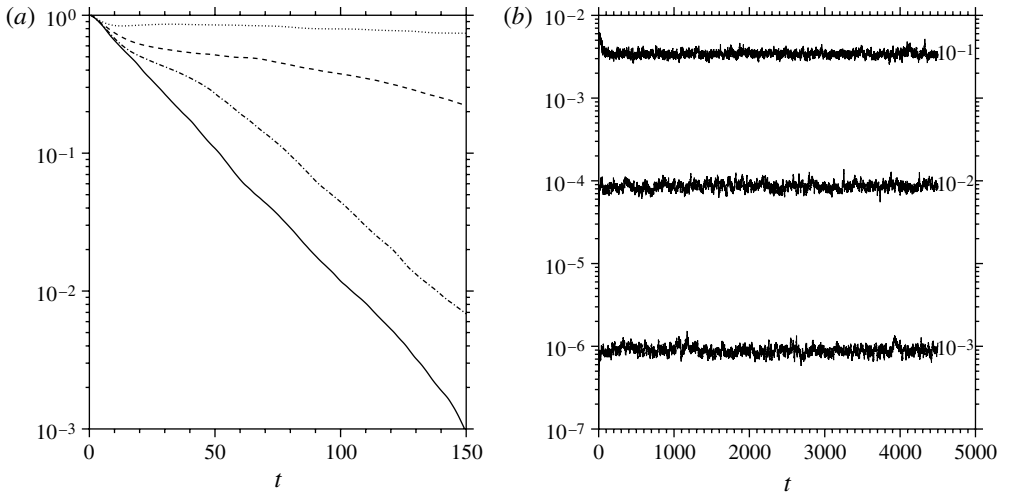

FIGURE 2. Method (i): time history of the normalized magnetic energy in the $(k, l) = (0, 1/2)$ component for $B_0 = 10^{-3}$ (solid) 10^{-2} (dot-dashed) 2×10^{-2} (dashed) 10^{-1} (dotted). The decay rates are computed by fitting a straight line to the later parts of the curves. Method (ii): time histories of the total magnetic energies for $B_0 = 10^{-3}$, 10^{-2}, 10^{-1}. The turbulent diffusivity is calculated from these curves using (3.5).

the respective driving frequencies is independent of $\hat{S}(k_y)$ and given by

$$\mathscr{R}(k_y) = \frac{|G_1(k_y)|^2}{|G_2(k_y)|^2} = \frac{\omega_1^2(\eta_T^2 k_y^4 + \omega_2^2)}{\omega_2^2(\eta_T^2 k_y^4 + \omega_1^2)}, \tag{3.11}$$

where the G_i are the Fourier coefficients of the solution corresponding to driving at frequency ω_i. This defines η_T for any value of k_y. Clearly $\mathscr{R}(k_y)$ can be calculated from turbulence calculations by Fourier analysis. However, the analogy between the averages of the solution of (3.2) and the averaged (3.3) is only valid if the assumptions about a sufficient separation of scales are valid. This has to be verified *a posteriori*: there is no way to know in advance whether the separation of scales remains valid in the presence of a mean field. These are best satisfied by the low wavenumbers rather than the high wavenumbers, and thus it makes sense to compute η_T from the lowest overtone k_{y_1}. Also we note that the expression on the right-hand side of (3.11) rapidly approaches unity for large k_y and therefore it would require knowledge of $\mathscr{R}(k_y)$ to high precision in order to compute η_T accurately. Thus, for the rest of this paper we shall use $\mathscr{R}(k_{y_1})$ to extract our working definition of η_T.

3.2.2. *Results*

We are now in a position to put these methods to the test. First of all, and for comparison, we calculate the diffusivity using methods (i) and (ii). Figure 2(*b*) shows time series of the (normalized) energy in the $k_y = k_{y_1}$ component of the magnetic field for the decay experiment of method (i), for four different choices of the initial magnetic field (B_0). This experiment is started from a solution of the hydrodynamic system once the dynamics has settled down to a statistically steady state. Even though there is noise in the data owing to the turbulent fluctuations the decay rate can be calculated by fitting the decaying solution. It is clear from the figure that the decay rate is diminished as the initial field strength is increased so that the magnetic field

is suppressing the turbulent diffusion (see Cattaneo & Vainshtein 1991). Figure 2(*b*) shows time series of the average magnetic energy for different values of an imposed mean field B_0. The turbulent diffusivity can be calculated in this case using method (ii) (specifically (3.5)) once the averages have converged.

The results of methods (i) and (ii) are shown as the diamonds and the solid line in figure 5, respectively. Here the values are shown as a function of the effective mean field B_0^e. How B_0^e is assigned is a delicate issue that we shall return to in the discussion. For now we note that the measured diffusivity for the two methods agree. This confirms that there is enough separation of scales between the typical eddy size and the system size for the concept of turbulent diffusivity to be valid. The values for weak fields gives the kinematic turbulent diffusivity ($\eta_T^{(0)}$); if one makes the reasonable assumption that this should be of the order UL where U is the root mean square (r.m.s.) velocity and L is the characteristic scale of the eddies, then $\eta_T^{(0)}/\eta \approx 180$ is an estimate of Rm for the turbulence. Since U is known, this gives an estimate of $L \approx 0.2 \ll 2\pi$, so the separation of scales is reasonable. Furthermore, according to common folklore (Cattaneo & Vainshtein 1991; Gruzinov & Diamond 1994) substantial departure from the kinematic value for the turbulent diffusivity should occur when $B_0 \sim O(1/Rm) \sim 5 \times 10^{-3}$ which is borne out by the numerical results in figure 5. For larger B_0 the turbulent diffusivity is quenched, eventually to reach its molecular value.

We can now turn to methods (iii) and (iv) to see whether they recover all (or any) of the above features. In what follows we shall consider three values of $\omega = 0.05, 0.1$ and 0.2. Our two methods correspond to two different choices for the source function. For the TAM, which is an approximation of a field localized near a boundary in an experiment we set

$$S_{TAM}(y) = B_0 \left[\exp\left(-\mu(y - Y_{mx}/4)^2\right) - \exp\left(-\mu(y - 3Y_{mx}/4)^2\right)\right]. \tag{3.12}$$

We have performed calculations with $\mu = 100$ and $\mu = 1000$, but have determined that for μ sufficiently large then the degree of localization does not matter.

The second choice of source function involves setting

$$S_{MOS} = B_0 \sin(2\pi y/Y_{mx}), \tag{3.13}$$

which is the largest-scale Fourier component that fits in the domain.

Figure 3 shows a typical snapshot density plot of B_x for the two different source functions after the initial transients have decayed away at the same phase of the calculation for a source term that is strong enough to be dynamic. These images shows the turbulence wrapping up the magnetic field, but the imprint of the source function is clearly visible at this time. As the driving alternates, the regions of white and black swap around. In order to calculate the diffusivity via the methods (iii) and (iv) we need to determine the x-average of B_x as a function of y and t for many cycles. The raw data for method (iii) therefore has the form of figure 4(*a*), which shows $\langle B_x \rangle(y, t)$ for two different frequencies of oscillation, this time for a kinematic case. Note these show only a small proportion of a typical calculation. Here one can clearly see the oscillations of the $k_x = 0$ component and the effect of the turbulence in spreading the magnetic field from the localized source.

The next step is to take the two-dimensional data and to extract the response of the system at the driving frequency ω and large spatial scales (small wavenumbers). Clearly this can be achieved by space–time Fourier analysis. In principle, it should not make any difference in which order the Fourier analyses are taken (either space

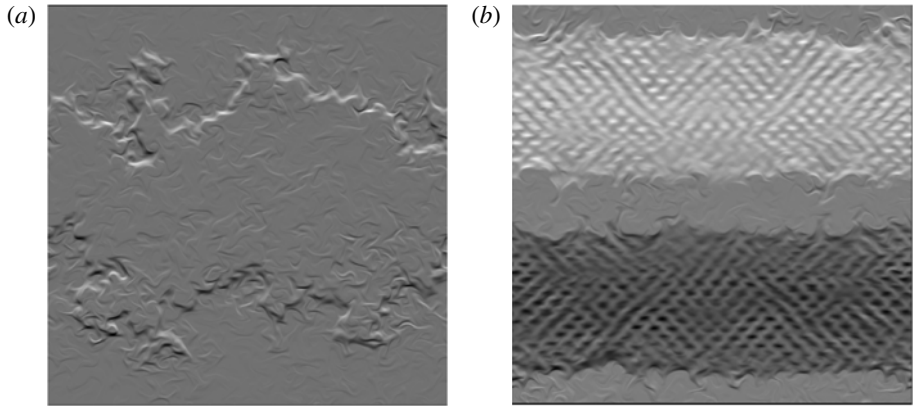

FIGURE 3. Density plots of B_x at a given time in the dynamic regime. (*a*) Method (iii) (TAM), where $\mu = 1000$. (*b*) Method (iv) (MOS).

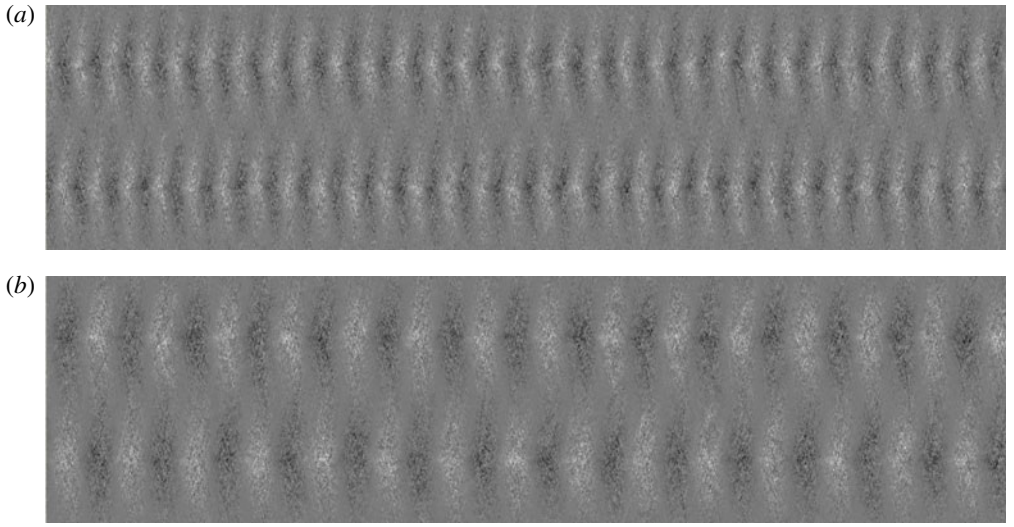

FIGURE 4. Space–time density plots of the x-average of B_x as a function of y (vertical) and t (horizontal) for method (iii) (TAM) in the kinematic regime: (*a*) $\omega = 0.1$ and (*b*) $\omega = 0.05$. Runs used to measure the diffusivity via Fourier analysis are typically 10 times longer than this sample.

then time or *vice versa*). In practice, here it is much better to do space first and time second. This is because the numerical solution is expressed in space at the Fourier collocation points, but that is not the case in time. Thus, if the time transform is performed first, then it can introduce errors that propagate through into the calculation of η_T. If the space transform is performed first then it is simple to remap the resulting one-dimensional series onto the collocation points of the temporal transform and minimize the errors. Once the space–time transform is performed we use (3.11) and

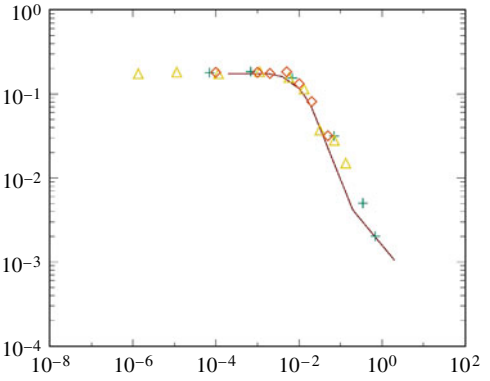

FIGURE 5. (Colour online) Measurements of the turbulent diffusivity for all methods described as a function of the effective large-scale field B_0^e. Method (i) is shown with diamonds, method (ii) is shown with a solid line, method (iii) (TAM) is shown with triangles and method (iv) is shown with crosses.

the fact that in our case $k_{y_1} = 1/2$ to obtain

$$\eta_T^2 = \frac{16\omega_2^2(\mathscr{R} - 1)}{1 - \omega_2^2\mathscr{R}/\omega_1^2}, \tag{3.14}$$

where $\mathscr{R}$ is $\mathscr{R}(1/2)$ from (3.11).

We perform calculations for each of methods (iii) and (iv) for three choices of frequency $\omega = 0.05$, 0.1 and 0.2 for a range of B_0 that goes from being kinematic to strong enough to suppress the diffusivity. For the TAM (with $\mu = 1000$) this B_0 takes the values 10^{-4}, 10^{-3}, 10^{-2}, 10^{-1}, 0.5, 1.0, 5.0, 10.0 and 50.0, whilst for the MOS B_0 takes the values 10^{-4}, 10^{-3}, 10^{-2}, 10^{-1}, 0.5 and 1.0. As noted earlier we also use two different degrees of localization for the TAM (i.e. values of μ) to determine sensitivity to the degree of localization. Clearly for each value of B_0 and each method there are three possible frequency ratios that can be used to compute η_T using (3.14). Our choices of ω_1 and ω_2 ensure that both of these frequencies are small compared with the characteristic frequency of the turbulence. Once these frequencies have been chosen, each calculation must be run for long enough so that there are enough cycles so that there is good frequency resolution at the low frequencies and the transient response has died away. This last requirement becomes particularly demanding when the field is strong and the effective diffusivity approaches the molecular value; see (3.8). If all of these conditions are satisfied, then this method is robust with respect to choices of frequency pairs.

The results of all of the methods are summarized in figure 5, which shows the value of the turbulent diffusivity as a function of the effective large-scale field B_0^e. A few comments are in order. All methods agree well in the kinematic regime. Moreover, all methods predict unambiguously the value of B_0^e at which substantial departure from kinematic behaviour first appears. As one would expect the greatest disagreement occurs for the largest values of B_0^e for which η_T is quenched to the molecular value and all of the error bars become large. Method (i) is particularly poor in this regime, since it relies on measuring the decay rate of a very slowly decaying signal in a turbulent environment.

We note that the kinematic diffusivity, as a calculated by all four methods, for this two-dimensional flow is exactly that for a passive scalar and therefore can be written as $\eta_T \sim U/k$. Interestingly if we choose the value $U = U_{rms}$ as measured in the simulations, then the observed value of η_T is recovered with k chosen to be the most energetic wavenumber. So these methods are not only consistent with each other but they agree with our expectation of what the kinematic diffusivity should be in the turbulent regime.

4. Discussion

We begin the discussion by noting that both the TAM and the MOS work and give results that are consistent with each other and with one's expectations of what a turbulent diffusivity should do. The careful reader will have noticed that we have already twice in this paper deferred the discussion of how B_0^e is related to the input value of B_0 for each method. We feel that we can defer no further. Clearly B_0^e is a measure of the large-scale field as perceived by the small-scale turbulence. One expects B_0^e to be monotonic in B_0 and in some cases it is even proportional to B_0. Now we describe in detail how it is defined for all of the methods. The starting point for us here is method (i) because it is the most natural: it is related to the effective decay rate of a large-scale field. For this case we set $B_0^e = B_0$: the value initially imposed large-scale field. The next easiest one to rationalize is the scaling for the MOS. Here we choose B_0^e to be the r.m.s. amplitude (measured in the stationary regime once the transients have decayed) of the largest-scale Fourier component. For this method this is not too dissimilar to (but not exactly equal to) the r.m.s. amplitude of the applied signal. The same method works for the TAM, but in this case the r.m.s. value of the largest-scale Fourier component is much smaller than the r.m.s. amplitude of the (extremely localized) applied signal. For method (ii) some thought is required. It is intuitively obvious that a uniform field of strength B_0 has a stronger influence on the turbulence than any other Fourier component of the same amplitude. However, intuition can only take you so far. The procedure we adopt is to set $B_0^e = \lambda B_0$ where λ is the ratio of the peak (in time) r.m.s. values of the magnetic field for the experiments with a uniform field and an initial large-scale field. In both cases the peak value is achieved within a few turnovers. Some comments may be useful in justifying this procedure. For these cases most of the magnetic energy is concentrated at wavenumbers that are close to the peak in the kinetic energy; therefore from the point of view of the turbulence, what matters is the amount of magnetic energy that is generated at those scales, the ratio of which is essentially given by λ (which in this case is a number of $O(2)$).

It is appropriate to comment about our choice of two-dimensional turbulence with all of its attendant peculiarities. We reiterate that the reason we chose to examine this system was not exclusively for computational convenience, but also because in two dimensions there are other (tried and somewhat trusted) methods for which comparison is possible. We expect that adapting this to three dimensions should not present any conceptual problems and we are currently implementing this method for three-dimensional convective flows.

We conclude with a couple of comments about the implementation of these methods. Numerically both the MOS and the TAM work; however, the former is easier to implement and so we recommend it. Here we choose a source function with a sinusoidal spatial distribution because sines and cosines are the natural choice for a Cartesian domain with uniform collocation points. In general, one should pick a

functional form for the source function that is 'close' to a low-order eigenfunction of the diffusion operator in whatever geometry is being used.

It is our hope that this paper will inspire measurement of the turbulent diffusivity in a laboratory setting; indeed, some have already been performed in run-down experiments (Frick *et al.* 2010; Noskov *et al.* 2012). We hope that some of the lessons we have learned here will prove useful in setting up such an experiment. An experimental set-up will be closer although not identical to the TAM. In an experiment one would impose time-dependent magnetic fields outside of the device, which would penetrate into the interior by an amount comparable to the skin depth. If the frequency of the oscillation is large enough, then in the absence of motion in the experiment the skin depth is short, and so the effects of the external magnetic field resembles a boundary term. This will be conceptually close to the TAM method with a localized source term. Measurements of the field inside the domain will be obtained by a relatively modest number of probes at strategic locations. Again, the position of the probes should, as above, be close to the natural collocation points of the lowest eigenfunctions of the diffusion operator. When comparing the dependence of the turbulent diffusivity on the applied magnetic field for two different experiments then many of the considerations discussed above will apply. Namely that the important quantity is the level of mean magnetization felt by the turbulent eddies that are responsible for the effective transport. This of course will vary according to geometry, forcing and other characteristics of the experiment. Care must therefore be taken in making universal statements based on the result of a single experiment.

Acknowledgements

We would like to thank C. Forest and J.-C. Thelen for useful discussions. This work was partially supported by the National Science Foundation sponsored Center For Magnetic Self-Organization at the University of Chicago.

REFERENCES

ÅNGSTRÖM, Å. J. 1861 Neue methode, das wärmeleitungsvermögen der körper zu bestimmen. *Ann. Phys. Chem.* **114**, 513–530.

BRANDENBURG, A., RÄDLER, K.-H., RHEINHARDT, M. & SUBRAMANIAN, K. 2008 Magnetic quenching of α and diffusivity tensors in helical turbulence. *Astrophys. J. Lett.* **687**, L49–L52.

BRANDENBURG, A., SVEDIN, A. & VASIL, G. M. 2009 Turbulent diffusion with rotation or magnetic fields. *Mon. Not. R. Astron. Soc.* **395**, 1599–1606.

CANUTO, C., HUSSAINI, M. Y., QUARTERONI, A. & ZANG, T. A. 1987 *Spectral Methods in Fluid Dynamics*. Springer.

CATTANEO, F. 1994 On the effects of a weak magnetic field on turbulent transport. *Astrophys. J.* **434**, 200–205.

CATTANEO, F. & HUGHES, D. W. 2009 Problems with kinematic mean field electrodynamics at high magnetic Reynolds numbers. *Mon. Not. R. Astron. Soc.* **395**, L48–L51.

CATTANEO, F. & VAINSHTEIN, S. I. 1991 Suppression of turbulent transport by a weak magnetic field. *Astrophys. J. Lett.* **376**, L21–L24.

COURVOISIER, A., HUGHES, D. W. & TOBIAS, S. M. 2009 Mean induction and diffusion: the influence of spatial coherence. *J. Fluid Mech.* **627**, 403.

EYINK, G. L. 2009 Stochastic line motion and stochastic flux conservation for nonideal hydromagnetic models. *J. Math. Phys.* **50** (8), 083102.

FRICK, P., NOSKOV, V., DENISOV, S. & STEPANOV, R. 2010 Direct measurement of effective magnetic diffusivity in turbulent flow of liquid sodium. *Phys. Rev. Lett.* **105** (18), 184502.

GRUZINOV, A. V. & DIAMOND, P. H. 1994 Self-consistent theory of mean-field electrodynamics. *Phys. Rev. Lett.* **72**, 1651–1653.

KRAUSE, F. & RAEDLER, K. H. 1980 *Mean-Field Magnetohydrodynamics and Dynamo Theory*. Pergamon.

MOFFATT, H. K. 1974 The mean electromotive force generated by turbulence in the limit of perfect conductivity. *J. Fluid Mech.* **65**, 1–10.

MOFFATT, H. K. 1978 *Magnetic Field Generation in Electrically Conducting Fluids*. Cambridge University Press, 353 p.

MONCHAUX, R., BERHANU, M., AUMAÎTRE, S., CHIFFAUDEL, A., DAVIAUD, F., DUBRULLE, B., RAVELET, F., FAUVE, S., MORDANT, N., PÉTRÉLIS, F., BOURGOIN, M., ODIER, P., PINTON, J.-F., PLIHON, N. & VOLK, R. 2009 The von Kármán sodium experiment: turbulent dynamical dynamos. *Phys. Fluids* **21** (3), 035108.

NOSKOV, V., DENISOV, S., STEPANOV, R. & FRICK, P. 2012 Turbulent viscosity and turbulent magnetic diffusivity in a decaying spin-down flow of liquid sodium. *Phys. Rev.* E **85** (1), 016303.

PARKER, E. N. 1979 *Cosmical Magnetic Fields: Their Origin and their Activity*. Clarendon; Oxford University Press, 858 p.

RICHARDSON, L. F. 1926 Atmospheric diffusion shown on a distance-neighbour graph. *Proc. R. Soc. Lond.* A **110**, 709–737.

SCHRINNER, M., RÄDLER, K.-H., SCHMITT, D., RHEINHARDT, M. & CHRISTENSEN, U. 2005 Mean-field view on rotating magnetoconvection and a geodynamo model. *Astron. Nachr.* **326**, 245–249.

TAYLOR, G. I. 1921 Experiments with rotating fluids. In *Proc. R. Soc. Lond.* , **100**, 114–121.

ZEL'DOVICH, YA. B. 1957 The magnetic field in the two-dimensional motion of a conducting turbulent fluid. *Sov. Phys. J. Expl Theor. Phys.* **4**, 460–462.